Korean J. Chem. Eng., 33(4), 1362-1368 (2016)
DOI: 10.1007/s11814-015-0228-2

pISSN: 0256-1115
eISSN: 1975-7220

Pilot-scale study on dehydration of synthetic and lignocellulosic ethanol by NaA membrane

Hwa-Jou Wei*,,†, Tsung-Yen Tsai*, and Yu-Hsiang Weng***,†**

*Institute of Nuclear Energy Research, Atomic Energy Council, Executive Yuan,
1000 Wenhua Rd., Jiaan Village, Longtan Township, Taoyuan County 325, Taiwan, ROC
**Department of Chemical and Materials Engineering, National Central University, Taoyuan 320, Taiwan, ROC
***Green Technology Research Institute, CPC Corporation, Taiwan, 2 Tsuo-Nan Rd., Kaohsiung 811, Taiwan, ROC
(*Received 20 October 2014 • accepted 6 November 2015*)

Abstract−A pilot scale vapor permeation unit was assembled to study the dehydration of bioethanols with NaA membrane. The operational parameters, such as feed concentration, temperature, and downstream pressure in permeate, were varied. Long-term operation of an ethanol dehydration unit was demonstrated. Additionally, the lingocellulosic ethanol distillate was dehydrated to fuel grade ethanol with less than 1% water content. The changes in impurities, such as methanol, ethylacetate, 2-propanol, 1-propanol, 1-butanol, and Isoamyl alcohol, were dependent on the volatility of the compounds. The ethanol concentrations in the permeate stream were lower than 1%, indicating high separation performance of the membrane system.

Keywords: Bioethanol, Vapor Permeation, Dehydration, Impurity, Inorganic Membrane

INTRODUCTION

Biofuels, such as biodiesel and bioethanol, have been paid great attention in recent years due to their renewability. In particular, lignocellulosic ethanol, which is produced from using lignocellulosic materials, has the advantages of abundance and non-food crop characteristics over ethanol produced from corn and sugar cane. However, cost-effective conversion of lignocellulosic biomass into ethanol is still a challenging task due to the lack of integrated process configurations. It is expected that lignocellulosic ethanol process via a biochemical route will be commercialized before 2020 [1,2].

The steps in the lignocellulosic ethanol production process include pretreatment (acid, base, high temperature, or high pressure), enzyme hydrolysis, ethanol fermentation, and ethanol purification [1,3-6]. The most common method for ethanol purification is distillation. However, the distillate, consisting of 90-95% of ethanol content, cannot meet fuel specifications [7]. Further purification steps, such as azeotropic distillation, molecular sieve adsorption, and membrane separation, are needed to remove residual water to less than 0.5% (v/v) and to raise the ethanol level to 99.3% (v/v) [4,8].

Membrane separation is an energy-saving process for dehydrating ethanol. However, most commercially available ethanol dehydration membranes are polymeric membranes [9,10]. Over the past decades, the interest in the development of inorganic membranes has increased. Specifically, the inorganic zeolite membranes appear to have much better thermal, chemical, and mechanical stability than polymeric membranes do, providing an alternative opportunity for industrial applications [11-13]. A successful demonstration by Mitsui Engineering and Shipbuilding Co. Ltd. showed that one potential method of alcohol dehydration could be to use NaA (or LTA) membrane [14].

Morigami et al. [14] showed that in a large-scale membrane plant, 90 wt% of ethanol was dehydrated by zeolite NaA membranes with a separation factor of up to 30,000. The tested feed solution included actual waste ethanol, IPA, and methanol. Further scaled up plants owned by Nano-Research Institute Inc. (a 100% subsidiary of Mitsui & Co.) achieved 3,000 L/d (in Brazil) and 30,000 L/d (in India) using the same membrane, demonstrating the promise of the technology [15]. Similarly, Richter et al. [16] reported that NaA membrane had high separation performance. In that study, both synthetic and industrial fermentation ethanols were tested. They found that similar permeation fluxes were obtained when the system was operated in pervaporation and vapor permeation modes.

Although ethanol dehydration by inorganic membranes has been demonstrated successfully on laboratory [17,18], pilot [19], and industrial scales [14,16], little has been reported about dehydration of lignocellulosic ethanol produced from agricultural wastes, especially from rice straw. Furthermore, detailed information about the composition of lignocellulosic ethanol is usually unavailable [20]. During ethanol production, other fermentation by-products (such as ethyl acetate, 1-propanol, and methanol) are generated simultaneously [21,22]. Concurrent dehydration of lignocellulosic ethanol containing these by-products would provide invaluable information on problems that would likely be encountered in an industrial-scale fuel-grade ethanol production process.

In this study, dehydration of ethanol was systematically studied by varying the feed ethanol concentration, feed temperature, and downstream pressure. Several batches of ethanol were dehydrated to demonstrate the stability of the system. Furthermore, lignocellu-

†To whom correspondence should be addressed.
E-mail: hwajou@iner.gov.tw, 078719@cpc.com.tw, f88541105@ntu.edu.tw

Table 1. Characteristics of the membrane used in this study

Parameter	Characteristics[a]
Configuration	Tubular
Material	Zeolite NaA
Filtration area (cm^2)	890
Tube length/diameter (cm)	120/2
Number of channel	4
Channel diameter (cm)	0.6
Maximum operational temperature (°C)	150
Maximum operational pressure (Bar)	10
Water content in feed (%)	<20%

[a]Data were taken from inocermic, Germany

losic ethanol obtained from a lignocellulosic ethanol pilot plant [4, 23,24] was dehydrated to further an understanding of the performance of the separation system.

MATERIALS AND METHODS

1. The Membrane and Separation System

NaA zeolite membrane (purchased from Inocermic GmbH, Germany) was used to study dehydration performance of synthetic and lignocellulosic ethanols. The NaA zeolite membranes were synthesized in the internal side of the tubular supports to offer best mechanical and hydrodynamic conditions [11]. Typically, a separation factor of 10,000 could be obtained [25], indicating high separation performance of the membrane. In this study, a single membrane module with an effective area of 890 cm^2 was used (see Table 1). The tube length and tube diameter are 120 and 2 cm, respectively. There are four channels in each tube. Additional membrane module can be incorporated when it is necessary [26]. Fig. 1 shows the schematic diagram of the pilot plant. The dehydration system consists of a high pressure feed pump, an evaporator, a membrane module, two coolers, and a vacuum pump. The system was operated in vapor permeation mode. Ceramic fiber blankets were wrapped on the tubing and housing of the membrane module to minimize the loss of heat to air. No additional heating was provided on the tubing.

2. Experiment Protocol

Single-pass continuous mode (i.e., no recycling of the concentrate) was conducted for dehydration of synthetic ethanol solution (91%-97%), while batch circulation mode (i.e., recycling of concentrate only) was adopted for dehydration of ethanol (85%-95%) and lignocellulosic ethanol solutions. When the temperature in the feed tank reached a desired value, the feed pump and the automatic control valve were turned on to start the experiment. Typical feed rate was 5 kg/h. The operational temperatures varied from 80 to 127 °C, corresponding to the gauge pressures of 0.1 to 4.6 bar. Temperature of the cooling trap on the permeate side was 2-10 °C. The system was equilibrated for about one hour before the data were collected. For the synthetic ethanol experiments, the time interval for each data point was more than 20 min. The feed solution samples were taken before they entered the evaporator. Ethanol product samples were taken from the outlet of membrane module. A control valve in the permeate side needs to be closed to allow taking permeate samples. The product and permeate streams were sampled simultaneously for chemical analyses and for determining flux. For the batch circulation mode experiments, ethanol concentration in the circulation tank was measured at selected intervals.

3. Lignocellulosic Ethanol

The lignocellulosic ethanol pilot plant consists of four units, including dilute acid hydrolysis pretreatment, enzymatic hydrolysis, fermentation and ethanol distillation [23,24]. The design capacity of the pilot plant is one ton of feedstock per day. Separate hydrolysis and fermentation (SHF) and simultaneous saccharification and fermentation (SSF) processes were studied in the test runs. Simultaneous saccharification and co-fermentation (SSCF) process can be applied after a glucose and xylose co-fermenting recombinant yeast is developed. The design criteria for the pilot plant were as follows: dilute acid pretreatment in continuous mode, 75%-80% ethanol yield without detoxification for C5 sugar and high solid/liquid ratio (20%-25%) with 75% ethanol yield for C6 sugar. The current feed stock is rice straw but flexible to sugarcane bagasse, hardwood, and other biomass.

The steam explosion pretreatment system was operated at 150-250 kg/h. The pretreated cake was then subjected to enzymatic hydrolysis with a dosage of 20-25 FPU/g-cellulose. Typical reaction time was 48 hours and final glucose concentration was 50 g/L. After separating of lignin from the hydrolyzed, fermentation was conducted with *Saccharomyces cerevisiae* in a 7,000 L fermenter. The resulting fermentation broth with ethanol concentration of 1.5%-3.0% was then subjected to distillation. The ethanol concentration

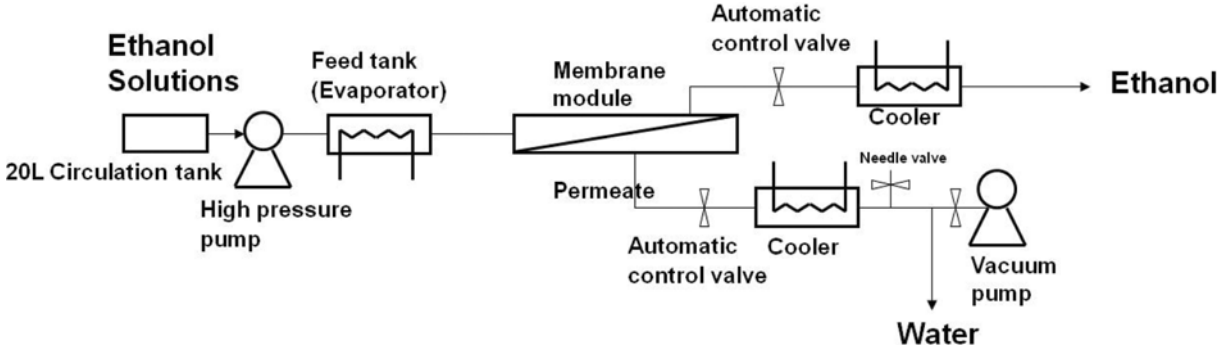

Fig. 1. The schematic diagram of a pilot scale ethanol dehydration system.

in the final distillate was 90%-94%.

4. Physical and Chemical Analyzes

The samples in the permeate stream were analyzed with high performance liquid chromatography (HPLC) to determine ethanol concentration. The chromatography analysis was performed on an 87H analysis column (Transgenomic Inc., USA) at 65 °C. 4 mM of H_2SO_4 solution was used as the mobile phase, flow rate was 0.8 mL min^{-1}, and the detection cell temperature in the RI detector was set at 45 °C. For each analysis, 20 μL of sample solution was injected into the system.

The samples in the feed and product streams were analyzed with a density meter (DA-130N, Kyoto Electronics) and gas chromatograph with flame ionization detector (GC/FID) to determine ethanol and the impurity content. A nonpolar HP-1 column with length of 100 meter was used. The conditions for analyses were as follows: injection temperature of 250 °C, split ratio of 50, column flow rate of 1 mL/min, and detection temperature of 300 °C.

Flux J (kg/m^2/h) can be determined with Eq. (1) where W is weight of solution in permeate side (kg), A is filtration area of membrane (m^2) and t is filtration time (h).

$$J = \frac{W}{At} \tag{1}$$

The separation factor was calculated according to Eq. (2).

$$\beta_{water/ethanol} = \frac{C_{water,\,per}/C_{ethanol,\,per}}{C_{water,\,feed}/C_{ethanol,\,feed}} \tag{2}$$

In Eq. (2), $C_{water,\,per}$ and $C_{ethanol,\,per}$ are the concentrations of water and ethanol in the permeate. $C_{water,\,feed}$ and $C_{ethanol,\,feed}$ are the concentrations of water and ethanol in the feed side.

To get the intrinsic membrane property but also better compare the present study with existing data set, membrane permeances (P_i^G/l) and selectivities ($\alpha_{water/ethanol}$) were calculated in addition to the parameters used above [27].

$$\frac{P_i^G}{l} = \frac{j_i}{p_{i_0} - p_{i_l}} \tag{3}$$

$$\alpha_{water/ethanol} = \frac{P_{water}^G/l}{P_{ethanol}^G/l} \tag{4}$$

where P_i^G is permeability (Barrers), l is membrane thickness (cm), j_i is molar flux (cm^3(STP)/cm^{2}s), p_{i_0} and p_{i_l} are the partial pressures of component i on either side of the membrane (cmHg), and P_{water}^G/l and $P_{ethanol}^G/l$ are the permeances of water and ethanol (gpu=10^{-6} cm^3(STP)/cm^{2}s cmHg). The NRTL model was used to calculate the partial pressures of ethanol and water.

RESULTS AND DISCUSSION

1. Effect of Feed Temperature on Separation Performance

To understand the characteristics of the membrane, dehydration of ethanol was conducted using a single membrane module. Single-pass continuous mode (i.e., no recycling of the concentrate) was conducted. Fig. 2 shows the ethanol product concentration at various operational temperatures. It is clear that ethanol product concentration increased as the feed temperature increased.

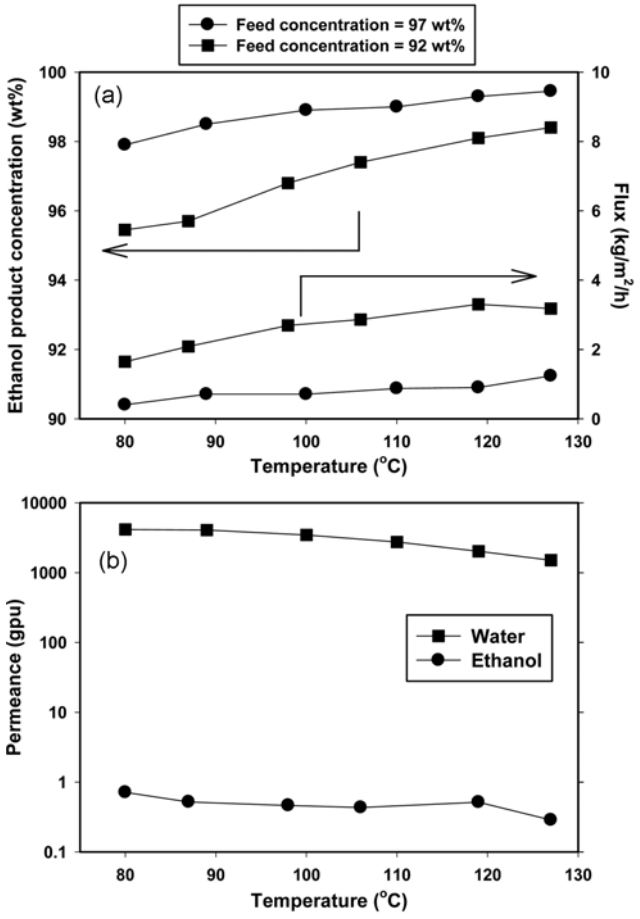

Fig. 2. (a) Ethanol product concentrations and permeate fluxes at various operational temperatures. (b) Water and ethanol permances at various operational temperatures. Feed ethanol concentration=92%. Downstream pressure=7-10 torr.

At feed ethanol concentration of 92%, ethanol product concentrations were 95.5% and 98.4%, when the feed temperature was at 80 and 127 °C, respectively. At feed ethanol concentration of 97% and 127 °C, the product concentration reached fuel grade level of 99.5%. Fig. 2 also shows that fluxes were from 1.6 to 3.2 kg/m^2/h at a feed ethanol concentration of 92%. Increasing the feed ethanol concentration from 92% to 97% decreased the permeation flux, representing a decrease in driving force (i.e., water content) for separation. A further analysis (Fig. 2(b)) shows that water permeance was greater than 1,000 gpu, but ethanol permeance was less than 1 gpu, resulting in high selectivity of the membrane (>4,000). Both the water and ethanol permeances decreased as the operational temperature increased. Note that the water permeance at 127 °C was about one-third of that at 80 °C. This phenomenon is similar to the study reported by Sato et al. [17] who showed that water permeance decreased with increasing of temperature from 100 to 145 °C with NaA membrane. However, Zah et al. [28] reported that the water permeance in the zeolite NaA layer increased as the temperature increased from 30 to 60 °C. In addition, Wang and Tsuru [29] found that both the water (~3,000 gpu) and ethanol (~0.6 gpu) permeances were approximately constant with increasing temperature from 40 to 75 °C by using Co-SiO_2 membranes.

The increase in flux with an increase in operational temperature was due to the increase in the vapor pressure across the membrane because the intrinsic membrane permeance decreased as the operational temperature increased. According to solution diffusion model, the membrane permeance is the combination of diffusion and sorption. Generally, the diffusion coefficient increases with increasing operational temperature, but sorption coefficient decreases with increasing temperature. The result in this study showed that the change in sorption was more significant than the change in diffusion. The differences in the results above may be due to the differences in the intrinsic properties of membranes and feed condition (VP vs. PV) employed. Additional study is needed to further elucidate the temperature dependent effect of water permeance during ethanol dehydration.

The analyses for the apparent activation energy for permeation flux through the membrane were conducted with the following equation:

$$J_i = J_0 \exp\left(-\frac{E_i}{RT}\right) \quad (5)$$

where J_i (kg/m^2/h) is the flux, J_0 (kg/m^2/h) is the pre-exponential factor, E_i (kJ/mole) is the apparent activation energy for permeation flux through the membrane, R (J/mole/K) is the gas constant, and T (K) is the temperature. The calculated $E_{ethanol}$ and E_{water} were 23.4 and 16.6 kJ/mole, respectively. It is reasonable that the apparent activated energy for water passing through membrane was lower than that for ethanol since NaA membrane is hydrophilic. However, E_{water} in this study is smaller than those reported values of 32-35 kJ/mole in the literature [30,31]. This may be due to different types of supports used in fabricating the membrane. For example, Sato et al. [17] showed that activation energies for asymmetric and monolayer supports during permeating ethanol solution were 20 and 31 kJ/mole, respectively. The authors suggested different permeating mechanisms involved in the separation.

2. Effect of Downstream Pressure on Separation Performance

Fig. 3(a) shows the effect of downstream pressures on the ethanol product concentration and permeate flux. The downstream pressure was adjusted by a needle valve. The lower the downstream pressure, the higher the ethanol product concentration was. Similarly, permeate flux increased as the absolute pressure in downstream decreased. In addition, the higher the feed temperature, the higher the ethanol product concentration and permeate flux could be obtained. Fig. 3(b) expresses the results in terms of permeance and driving force across the membrane. The partial pressure difference across membrane for ethanol is much higher than that for water because there are differences in the volatility of water and ethanol. Generally, the vapor permeation is operated at higher temperature in comparison to pervaporation. Therefore, the partial pressure difference across membrane did not change much when the downstream pressure was adjusted. However, caution must be taken when the system is operated at low temperature. In such a case, feed vapor pressure is low and therefore the changes in downstream pressure would significantly influence the driving force for separation. Fig. 3(b) also shows that ethanol permeance was approximately unchanged at temperature of 80-120 °C, whereas water permeance decreased as temperature increased.

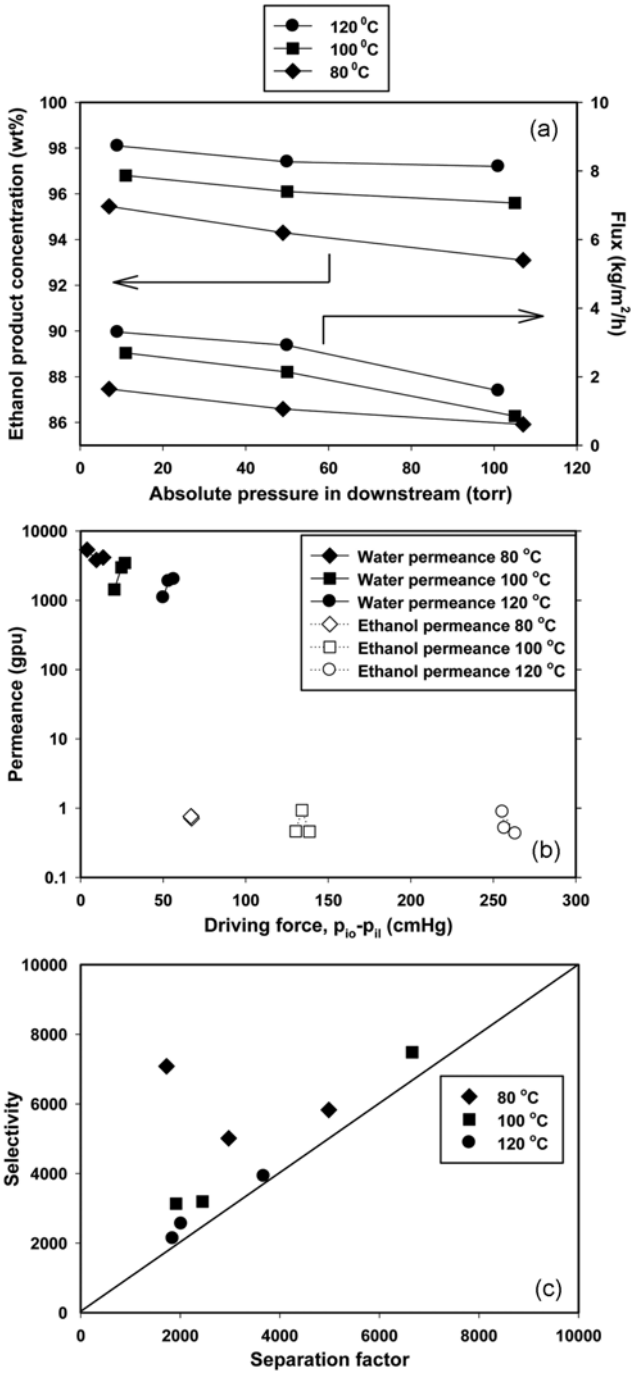

Fig. 3. (a) Ethanol product concentrations and permeate fluxes as a function of downstream pressure. (b) Water and ethanol permeances varied with driving forces. (c) The separation performance. Feed concentration=92 wt%.

Fig. 3(c) demonstrates separation factors and selectivities of water over ethanol at various downstream pressures and temperatures. Generally, the separation factor was proportional to selectivity. To get an intrinsic membrane property that does not depend on the operating conditions of the experiments, selectivity is preferred [27]. It is also recommended that the molar-based term is better than the mass-based one. Since permeates were rich in water

Table 2. Comparison of membrane performance for the dehydration of ethanol

Membrane	Ethanol in the feed (%)	Temperature (°C)	Flux ($g/m^2/h$)	Water in permeate (%)	Water permeance (gpu)	Selectivity $\alpha_{water/ethanol}$	References
Zeolite NaA	92	80	1,643	99.78	4,100	5,800	This study
Zeolite NaA	92	87	2,085	99.84	4,000	7,800	This study
Zeolite NaA	92	98	2,692	99.83	3,400	7,400	This study
Zeolite NaA[a]	90	90	2,500	99.8	3,600	5,100	Sommer and Melin [32]
Zeolite NaA[a]	90	110	4,900	99.9	3,500	10,000	Sommer and Melin [32]
Zeolite NaA[a]	90	75	2,150	>99.9	5,700	>10,000	Okamoto et al. [31]
Zeolite NaA[a]	90	105	4,500	99.97	3,800	33,000	Okamoto et al. [31]
PVA	85.1	98	-	-	710	100	Niemisto et al. [33]
CE	>95	75	-	-	~5,000	~500	Baker et al. [27]

PVA: polyvinyl alcohol, CE: cellose ester composite
[a]The permeate pressure is assumed to be a hard vacuum

(>99% water in all cases), separation factors and selectivities were high ranging from 1,700 to 6,600 and 2,100 to 7,400, respectively. Table 2 compares the performance of membrane for ethanol dehydration. The water permeance in this study was similar to those reported values using NaA membrane. However, due to higher ethanol permeances, the selectivities of 5,800-7,800 were lower than those values reported in the literature [31,32]. Nevertheless, NaA membrane performs much better than most commercially available organic membrane in terms of selectivity [27,33].

3. Continuous Dehydration of Ethanol in Batch Mode

To better understand long term stability of the dehydration system, seven batches of experiments were conducted continuously. Each batch lasted for more than 20 hr and the total operational time was 171 hr (see Fig. 4). The initial ethanol concentrations in the circulation tank ranged from 85% to 95%. The operational temperature and inlet pressure were 90 °C and 0.6 bar, respectively. The results showed that there was a sharp increase in ethanol product concentration in the beginning phase of filtration. The changes in ethanol product concentration with time gradually decreased when the ethanol product concentration was greater than ~95%. This was due to a decrease in the driving force (water con-

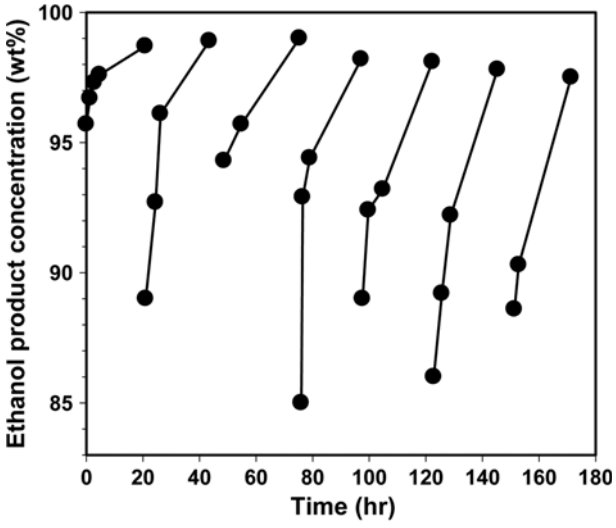

Fig. 4. Continuous dehydration of ethanol in batch mode. The operational temperature and inlet pressure were 90 °C and 0.6 bar, respectively.

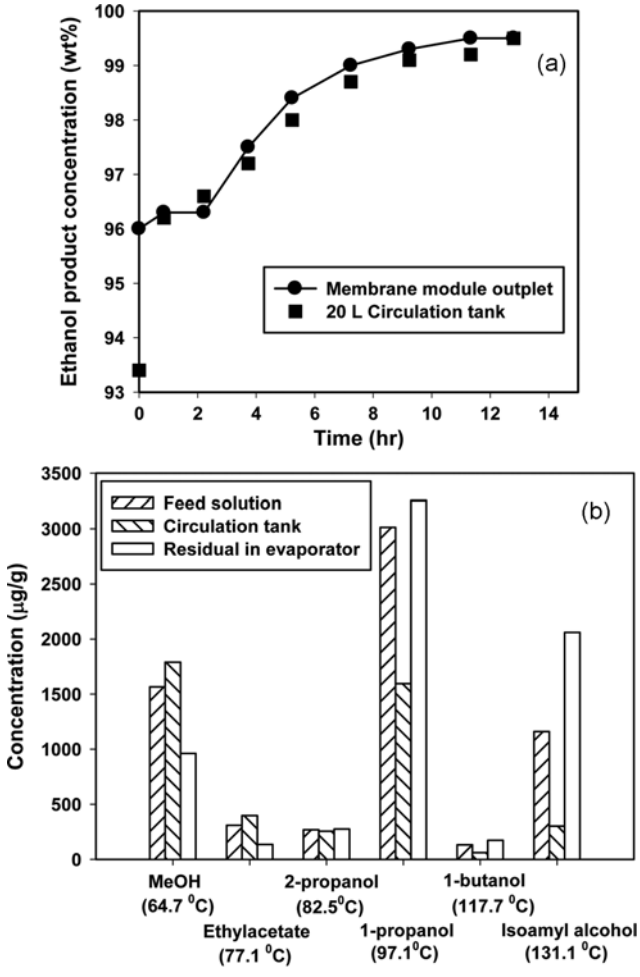

Fig. 5. Dehydration of lignocellulosic ethanol in batch mode. Experimental conditions: 100 °C, 1.4 bar, feed rate 6 L/h; downstream pressure 5-7 torr. (a) Changes in ethanol concentration with time. (b) Impurities in lignocellulosic ethanol.

tent) as the filtration proceeded. Final ethanol product concentration in the circulation tank increased to more than 98% in all the cases. The results provided a benchmark for studying the dehydration of lignocellulosic ethanol from rice straw.

4. Dehydration of Ethanol Solution Produced from Rice Straw

The lignocellulosic ethanol used in this study was obtained from a pilot plant in which rice straw was used as feed stock [23,24]. The rice straw was cut into small pieces and then subjected to hydrolysis. Dilute acid and enzyme catalyzed hydrolysis processes were employed. The resulting solution containing high sugar concentration was sent to fermentation. A broth with 1.5%-3.0% ethanol solution was obtained and then distilled to ca. 90% ethanol solution. Fig. 5(a) shows the changes in ethanol product concentration with time for a batch circulation experiment at 100 °C. The initial ethanol concentration was 93.4% after distillation. The start-up ethanol product concentration at membrane module outlet was 96%, which was close to a quasi-steady state value of 96.8% when synthetic ethanol was subjected to vapor permeation under similar experimental condition (see Fig. 2(a)). The ethanol concentration in the circulation tank increased sharply to 96.2% after 1 hr, and then gradually increased to 99.5% after 13 hrs of operation. The ethanol concentration in the permeate was below 0.5%. Note that dehydration rate decreased as the water content in the solution decreased. The overall mass recovery of the liquid was 98%, indicating that small amount of uncondensed vapor was lost.

Fig. 5(b) shows the profile of impurities in the lignocellusic ethanol before and after treatment. The detected compounds included methanol, ethylacetate, 2-propanol, 1-propanol, 1-butanol and Isoamyl alcohol. These alcohols and ester are common fermentation by-products found during ethanol production [21,22,34,35]. For example, ethyl acetate, 1-propanol, methanol, etc. were found during fermentation of grape must [21]. Fadeev et al. [22] found that glycerol, butanediols, butanols, propanols, etc. were generated during glucose fermentation. Note that those compounds with relatively high boiling points (~200 °C), such as glycerol and butanediols, were less likely to be present in the distillate after distillation. Organic impurities found in lignocellulosic ethanol were produced from empty fruit bunches (EFBs) of oil palm fiber included acetaldehyde, acetone, ethyl acetate, methanol, isopropyl alcohol , n-propyl alcohol, isobutanol and isoamyl alcohol [35].

The changes in composition of impurities depended on the volatility of the compound. 1-propanol and methanol were the major impurities in the feed ethanol, representing 47% and 24% of total impurity, respectively. Due to the differences in boiling point (1-propanol B.P.=97.1 °C, methanol B.P.=64.7 °C), methanol dominated the impurity in the product ethanol (i.e., in circulation tank) instead and its concentration increased from 1,567 to 1,789 mg/g (~0.18%). Note that high methanol concentration (>0.0236%) may lead to corrosive problems [35]. This could be solved by using a further step of distillation process. On the other hand, the concentration of 1-propanol in the product ethanol decreased from 3014 to 1596 mg/g, i.e., the proportion in the impurity decreased from 47% to 36%. Similarly, the concentrations of less volatile compounds (1-butanol and Isoamyl alcohol) in the product ethanol dropped significantly. Overall, the total amount of impurity decreased from 0.64% to 0.44% in the feed and product ethanols, respectively. The concentrated higher alcohols in the residual ethanol can be further separated after several batches of operation.

CONCLUSIONS

A pilot scale ethanol dehydration system was established for upgrading ethanol to fuel grade level. The results showed that NaA membranes could separate water from ethanol successfully. Typical permeate ethanol concentration was below 1%, indicating high separation performance of the system. The system was operated continuously for more than one week, demonstrating the stability of the process. Furthermore, lignocellulosic ethanol produced from rice straw was dehydrated from 93.4% to more than 99.3%. Caution must be taken when the methanol concentration is increased in refined bioethanol. The information obtained in this study gives a benchmark for scaling up a membrane dehydration facility.

ACKNOWLEDGEMENTS

This work was partly supported by a research grant, 99-2001-02-04-12, from the Atomic Energy Council of the Republic of China, Taiwan.

REFERENCES

1. E. Gnansounou and A. Dauriat, *Bioresour. Technol.*, **101**, 4980 (2010).
2. V. Menon and M. Rao, *Prog. Energy Combust. Sci.*, **38**, 522 (2012).
3. B. Klinpratoom, A. Ontanee and C. Ruangviriyachai, *Korean J. Chem. Eng.*, **32**, 413 (2015).
4. Y. H. Weng, H. C. Huang, G. L. Guo and W. S. Hwang, *J. Energy Power Eng.*, **5**, 928 (2011).
5. J. S. Lim, Z. A. Manan, S. R. W. Alwi and H. Hashim, *Renew. Sust. Energ. Rev.*, **16**, 3084 (2012).
6. S. Khan, M. Ul-Islam, W. A. Khattak, M. W. Ullah, B. Yu and J. K. Park, *Korean J. Chem. Eng.*, **32**, 694 (2015).
7. H. J. Huang, S. Ramaswamy, U. W. Tschirner and B. V. Ramarao, *Sep. Purif. Technol.*, **62**, 1 (2008).
8. CNS 15109, *Denatured fuel ethanol for blending with gasolines for use as automotive spark-ignition engine fuel* (2007).
9. R. W. Baker In *Membrane Technology and Applications*, 2nd Ed., Baker, R. W., Ed., John Wiley & Sons Ltd.: West Sussex (2004).
10. L. Y. Jiang, Y. Wang, T. S. Chung, X. Y. Qiao and J. Y. Lai, *Prog. Polym. Sci.*, **34**, 1135 (2009).
11. S. L. Wee, C. T. Tye and S. Bhatia, *Sep. Purif. Technol.*, **63**, 500 (2008).
12. L. M. Vane, *Sep. Sci. Technol.*, **48**, 429 (2013).
13. P. Peng, B. L. Shi and Y. Q. Lan, *Sep. Sci. Technol.*, **46**, 234 (2011).
14. Y. Morigami, M. Kondo, J. Abe, H. Kita and K. Okamoto, *Sep. Purif. Technol.*, **25**, 251 (2001).
15. J. Caro, M. Noack and P. Kolsch, *Adsorpt.-J. Int. Adsorpt. Soc.*, **11**, 215 (2005).
16. H. Richter, I. Voigt and J. T. Kuhnert, *Desalination*, **199**, 92 (2006).
17. K. Sato, K. Sugimoto and T. Nakane, *J. Membr. Sci.*, **307**, 181 (2008).
18. K. Shafiei, S. G. Pakdehi, M. K. Moghaddam and T. Mohammadi, *Sep. Sci. Technol.*, **49**, 797 (2014).
19. H. Z. Li, J. Q. Wang, J. Xu, X. D. Meng, B. Xu, J. H. Yang, S. Y. Li, J. M. Lu, Y. Zhang, X. L. He and D. H. Yin, *J. Membr. Sci.*, **444**, 513

(2013).
20. C. Abels, F. Carstensen and M. Wessling, *J. Membr. Sci.*, **444**, 285 (2013).
21. L. V. Reddy, L. P. Reddy, Y. J. Wee and O. V. S. Reddy, *Food Bioprocess Technol.*, **4**, 142 (2011).
22. A. G. Fadeev, S. S. Kelley, J. D. McMillan, Y. A. Selinskaya, V. S. Khotimsky and V. V. Volkov, *J. Membr. Sci.*, **214**, 229 (2003).
23. W. H. Chen, C. C. Tsai, C. F. Lin, P. Y. Tsai and W. S. Hwang, *Bioresour. Technol.*, **128**, 297 (2013).
24. T. H. Lin, C. F. Huang, G. L. Guo, W. S. Hwang and S. L. Huang, *Bioresour. Technol.*, **116**, 314 (2012).
25. Inocermic GmbH company, http://www.ikts.fraunhofer.de/en/research_fields/Environmental_EngineeringandBioenergy/biofuels.html (2014).
26. Y.-H. Weng, T.-Y. Tsai and H.-J. Wei, TW M425125 (2011).
27. R. W. Baker, J. G. Wijmans and Y. Huang, *J. Membr. Sci.*, **348**, 346 (2010).
28. J. Zah, H. M. Krieg and J. C. Breytenbach, *J. Membr. Sci.*, **284**, 276 (2006).
29. J. H. Wang and T. Tsuru, *J. Membr. Sci.*, **369**, 13 (2011).
30. C. H. Cho, K. Y. Oh, S. K. Kim, J. G. Yeo and Y. M. Lee, *J. Membr. Sci.*, **366**, 229 (2011).
31. K. Okamoto, H. Kita, K. Horii, K. Tanaka and M. Kondo, *Ind. Eng. Chem. Res.*, **40**, 163 (2001).
32. S. Sommer and T. Melin, *Chem. Eng. Sci.*, **60**, 4509 (2005).
33. J. Niemisto, A. Pasanen, K. Hirvela, L. Myllykoski, E. Muurinen and R. L. Keiski, *J. Membr. Sci.*, **447**, 119 (2013).
34. W. Osorio-Viana, J. D. Quintero-Arias, I. Dobrosz-Gomez, J. Fontalvo and M. A. Gomez-Garcia, *Desalin. Water Treat.*, **51**, 2377 (2013).
35. D. Styarinia, Y. Aristiawana, F. Auliaa, H. Abimanyua and Y. Sudiyania, *Energy Procedia*, **32**, 153 (2013).